Optimizing the Lateral Wandering of Automated Vehicles to Improve Roadway Safety and Pavement Life

December 2019 | Final Report

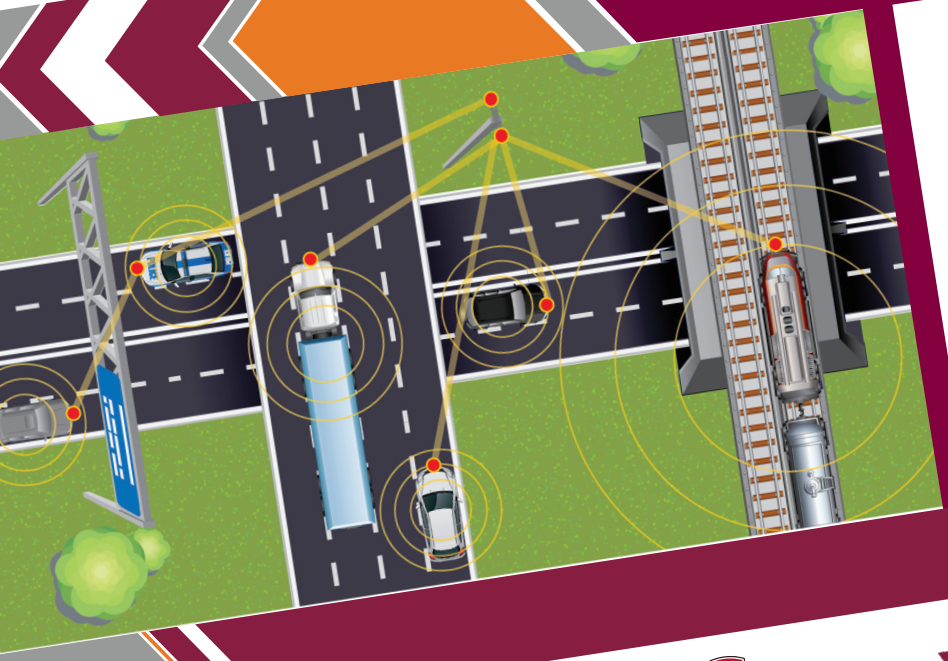

SAFE-D
SAFETY THROUGH DISRUPTION

Texas A&M Transportation Institute

San Diego State University
Leadership Starts Here

VT | TRANSPORTATION INSTITUTE
VIRGINIA TECH

Disclaimer

The contents of this report reflect the views of the authors, who are responsible for the facts and the accuracy of the information presented herein. This document is disseminated in the interest of information exchange. The report is funded, partially or entirely, by a grant from the U.S. Department of Transportation's University Transportation Centers Program. However, the U.S. Government assumes no liability for the contents or use thereof.

TECHNICAL REPORT DOCUMENTATION PAGE

1. Report No. 02-008	2. Government Accession No.	3. Recipient's Catalog No.
4. Title and Subtitle Optimizing the Lateral Wandering of Automated Vehicles to Improve Roadway Safety and Pavement Life		5. Report Date December 2019 6. Performing Organization Code:
7. Author(s) Fujie Zhou Sheng Hu Wenjing Xue Gerardo Flintsch		8. Performing Organization Report No. Report 02-008
9. Performing Organization Name and Address: Safe-D National UTC Texas A&M Transportation Institute		10. Work Unit No. 11. Contract or Grant No. 69A3551747115/Project 02-008
12. Sponsoring Agency Name and Address Office of the Secretary of Transportation (OST) U.S. Department of Transportation (US DOT) State of Texas		13. Type of Report and Period Final Research Report 14. Sponsoring Agency Code
15. Supplementary Notes This project was funded by the Safety through Disruption (Safe-D) National University Transportation Center, a grant from the U.S. Department of Transportation – Office of the Assistant Secretary for Research and Technology, University Transportation Centers Program, and, in part, with general revenue funds from the State of Texas.		

16. Abstract

Because most automated vehicles (AVs) are programmed to follow a set path and maintain a lateral position in the center of the lane, over time significant pavement rutting will occur. This study directly measured AV lateral wandering patterns. It was found that the wandering patterns of both AVs and human-driven vehicles could be modeled with a normal distribution but have significantly different standard deviations, with AV lateral wandering being at least 3 times smaller than the wandering of human-driven vehicles. Modeling with the Texas Mechanistic-Empirical Flexible Pavement Design System (TxME) found that the AVs with smaller lateral wandering would shorten pavement fatigue life by 22 percent and increase pavement rut depth by 30 percent, which leads to a much higher risk of hydroplaning. Researchers also calculated the maximum tolerable rut depths at different hydroplaning speeds. AVs have a much smaller tolerable rut depth than human-driven vehicles due to greater water film thickness in the rutted wheel paths. To reduce the negative impact of AVs on roadway safety and pavement life, this research recommends an optimal AV wandering pattern, a uniform distribution, which results in prolonged pavement life and decreased hydroplaning potential.

17. Key Words Automated Vehicle, Channelized, Normal Distribution, Uniform Distribution, Rutting, Fatigue Cracking	18. Distribution Statement No restrictions. This document is available to the public through the Safe-D National UTC website, as well as the following repositories: VTechWorks, The National Transportation Library, The Transportation Library, Volpe National Transportation Systems Center, Federal Highway Administration Research Library, and the National Technical Reports Library.

19. Security Classif. (of this report) Unclassified	20. Security Classif. (of this page) Unclassified	21. No. of Pages 30	22. Price $0

Abstract

Because most automated vehicles (AVs) are programmed to follow a set path and maintain a lateral position in the center of the lane, over time significant pavement rutting will occur. This study directly measured AV lateral wandering patterns. It was found that the wandering patterns of both AVs and human-driven vehicles could be modeled with a normal distribution but have significantly different standard deviations, with AV lateral wandering being at least 3 times smaller than the wandering of human-driven vehicles. Modeling with the Texas Mechanistic-Empirical Flexible Pavement Design System (TxME) found that the AVs with smaller lateral wandering would shorten pavement fatigue life by 22 percent and increase pavement rut depth by 30 percent, which leads to a much higher risk of hydroplaning. Researchers also calculated the maximum tolerable rut depths at different hydroplaning speeds. AVs have a much smaller tolerable rut depth than human-driven vehicles due to greater water film thickness in the rutted wheel paths. To reduce the negative impact of AVs on roadway safety and pavement life, this research recommends an optimal AV wandering pattern, a uniform distribution, which results in prolonged pavement life and decreased hydroplaning potential.

Acknowledgements

This project was funded by the Safety through Disruption (Safe-D) National University Transportation Center, a grant from the U.S. Department of Transportation – Office of the Assistant Secretary for Research and Technology, University Transportation Centers Program, and, in part, with general revenue funds from the State of Texas.

The authors appreciate the assistance of Mr. Yangwoo Kim and Dr. Alireza Talebpour in measuring AV lateral wandering. We also acknowledge Dr. Paul Carlson of Road Infrastructure, Inc. for reviewing and commenting on the report.

Table of Contents

List of Figures

List of Tables

Introduction

Significant innovation within the auto industry has brought an upcoming transportation revolution. Automated vehicles (AVs), including both cars and trucks, are coming at a rapid pace. In the last five years, AVs have gained substantial attention around the world, and autonomous technology is transforming both people's lives and the vehicle industry. Many car and commercial truck companies are dedicating significant resources and effort to improving automation. The potential benefits of deploying AVs have been widely discussed. These include reduction of congestion and traffic accidents, increased lane capacity, lower fuel consumption, increased transport accessibility, and reduced travel time and transportation costs [1]. However, one aspect of AVs that has not received enough attention is their potential impact on pavement rutting, the subsequent risk of vehicle hydroplaning, and ultimately on the lifespan of the roadway. Because more than 90% of commodities are transported by roadway in the United States, roadway infrastructure and associated safety issues play an essential role in our daily life. State Departments of Transportation (DOTs) spend billions of dollars annually to fix damaged roads [2]. Thus, it is crucial to investigate the impact of AVs on the risk of hydroplaning and roadway infrastructure life.

Background

AV Lane Use

There are many differences between AVs and human-driven vehicles. From the pavement perspective, one of the most apparent is how AVs position themselves within a traffic lane. AVs equipped with advanced positioning systems often can keep their position within the lane more precisely than human-driven vehicles. Accordingly, AVs have much less lateral wandering, which generally induces more damage to pavements in terms of rutting and cracking [3, 4, 5]. However, the pavement cracking and deeper rutting caused by AVs and associated hydroplaning potential have not been well investigated or quantified. This is due to the lack of detailed lateral wandering information on AVs available in the literature. Further investigation of this topic has the potential to decrease the risk of crashes related to hydroplaning, as well as lessen the cost of future roadway repair. Each year, about 37,000 people die in car crashes, 12 percent of which involve hydroplaning [6]. In addition, shortened pavement life and vehicle damages due to hydroplaning have significant economic cost.

Research Goal

The goal of this study was to investigate the impact of AV lane use and lateral positioning on wheel path cracking and rutting, as well as associated safety issues, and then develop guidelines on how AVs can best use traveling lanes to minimize safety concerns. This report first discusses the technologies used for AV lane keeping and then presents measured AV lateral wandering data. The authors then quantify the negative impact of AVs on pavement life (cracking and rutting) using the measured lateral wandering data. Furthermore, AV-related roadway hydroplaning is

discussed. To reduce the negative impact of AVs on pavement life and to improve the roadway safety of AVs, an optimal lateral wandering pattern for AVs is recommended at the end of this report.

Method

The study method included (1) quantifying AV lateral wandering based on the Texas A&M University's AV data; (2) determining the impact of AVs on pavement life in terms of rutting and cracking performance using mechanistic-empirical pavement design and analysis software; (3) evaluating the impact of AVs on hydroplaning potential according to widely accepted hydroplaning prediction models; and (4) recommending an optimized AV lateral wandering pattern to improve pavement life and safety.

Quantification of AV Lateral Wandering

Lane following and lane keeping are among the core features required to ensure safe and efficient autonomous driving. Overall, there are two types of lane keeping technologies: machine vision and Global Positioning System (GPS). Despite various techniques and algorithms presented in the literature and utilized by the AV industry, the main objective is to keep the AV within the lane with minimum deviation from the center. In general, any lane-keeping process has the following steps:

(1) Lane detection: Lane detection can be based on traditional machine vision approaches (e.g., utilizing various filters to determine lane color contrast) or deep learning approaches (e.g., R-CNN [7]). Regardless of the method, the result is a clear determination of the lane lines.

(2) Localization: This step is focused on identifying the AV's current position with respect to the lane and includes identifying the deviation from the center of the lane as well as lane curvature (required for the next step).

(3) Control: Once both the position of the vehicle within the lane and lane curvature are known, the vehicle's lateral controller ensures that the AV stays in the center of the lane. In case of deviation from the center, it ensures that the AV returns to the center as fast as possible while considering the maximum lateral acceleration.

Note that the only exception to this process is end-to-end deep learning-based lane-following [8], where the vehicle learns to stay within the lanes based on the observation of previous driving instances.

This study utilized the Texas A&M University's AV for data collection. This vehicle uses the three steps above for lane following. The lateral controller being implemented for the AutoDrive Project (a three-year competition to develop a fully automated vehicle sponsored by General Motors and SAE International) consists of a feedforward and feedback controller algorithm. The feedforward controller takes waypoint data, vehicle position, and velocity to determine the steering angle needed to follow the predetermined waypoints. The feedback controller takes the vehicle's

position, heading, and yaw rate and adjusts them to those of the path and corrects the steering angle based on the comparison. In other words, the feedforward portion of the controller determines the main component of the steering output, while the feedback portion modifies this predictive portion to account for any error in the vehicle's dynamic attributes. Utilizing the dynamic properties of a bicycle model, the feedforward controller can be represented as:

$$\delta_{ff} = \frac{L}{R} + K_{sg}\left(\frac{V^2}{gR}\right) \quad (1)$$

where δ_{ff} is the wheel angle, L is the vehicle wheel base, R is the radius of the curvature of the smooth path towards the center of the lane, V is the vehicle longitudinal velocity, and K_{sg} is the model parameter to be estimated. The feedback controller, on the other hand, comprises three components: lateral error, heading error, and yaw rate error.

$$\delta_{fb} = K_{lat}E_{lat} + K_{head}E_{head} + K_{omega}E_{omega} \quad (2)$$

where δ_{fb} is the wheel angle and E_{lat}, E_{head}, and E_{omega} are, respectively, errors in lateral position, heading, and yaw rate. K_{lat}, K_{head}, and K_{omega} are model parameters to be estimated.

Utilizing the above lane keeping algorithm, several experiments were conducted at the Texas A&M RELLIS campus (see Figure 1). The RELLIS campus is a World War II Air Force base that is being utilized as research and educational campus by the Texas A&M University.

Figure 1. Photo. Test location marked with red dashed line.

Lane keeping data were collected from autonomous driving along a 1-mile straight section of road with multiple straight lanes demarcated with clear lane markings. A constant driving speed of 20 mph along a straight lane was used when measuring lateral AV wandering. The data were collected at 3 Hz. The collected data were then compared with a human driver's lane keeping behavior to identify the difference between AVs and human drivers in this regard.

Impact of AVs on Pavement Life

Pavement life is influenced by four main factors: climate, traffic, pavement structure and subgrade, and the mechanical properties of each pavement layer material. Since the focus of this study is the impact of AV traffic on pavement life, all factors were kept the same, except for the factor of traffic, for all analyses and comparisons. In this study, the most significant difference between human-driven vehicles and AVs is the lateral wandering within a travel lane. Thus, the traffic volume and the weight of AV traffic were fixed in the analyses. The only variable of the analyses is the lateral wandering of AV traffic and its effect on pavement life in terms of fatigue cracking and pavement rutting.

For human-driven trucks, the edge of the truck tire is approximately 450 mm (18 in.) away from the lane markings, and regular trucks wander within a lane following a normal distribution (see Figure 2) with a standard deviation of 250 mm (10 in.) [9].

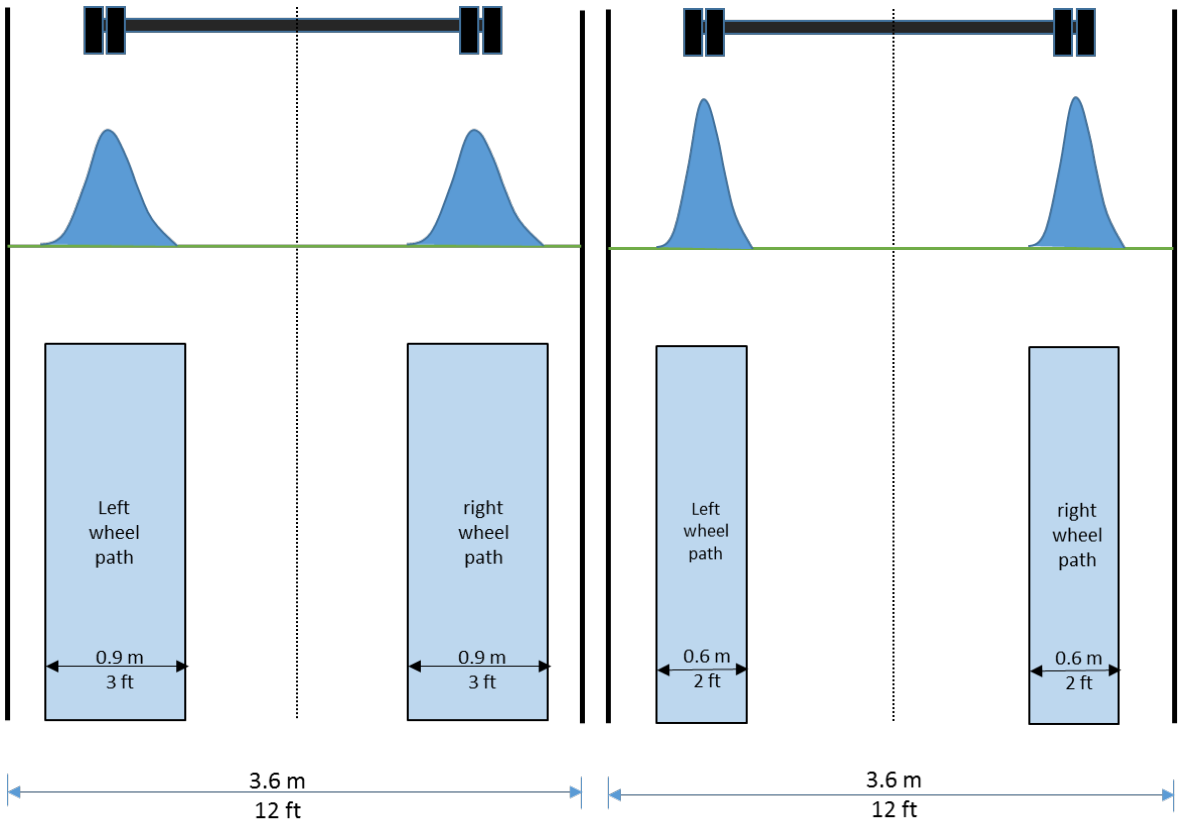

(a) Human-driven traffic (b) AV traffic

Figure 2. Diagram. Traffic wandering pattern: human-driven traffic vs. AV traffic.

For comparison, a normal distribution with a standard deviation of 75 mm (3 in.) for AV lateral wandering was chosen for this study. This is a safe estimate for the lateral wandering of AVs. Note that the wheel path width of AV traffic, as shown in Figure 2, is determined based on the tire-pavement contact width and the corresponding standard deviation of the lateral wandering.

This study employed a typical pavement structure (shown in Figure 3) to analyze the influence of lateral wandering on pavement fatigue cracking and rutting. It is assumed that such a pavement structure, located at Austin, Texas, will carry 30 million equivalent single axle loads (ESALs) within a 20-year design period. The typical pavement structure was subjected to two scenarios: 100 percent human-driven truck traffic and 100 percent AV truck traffic.

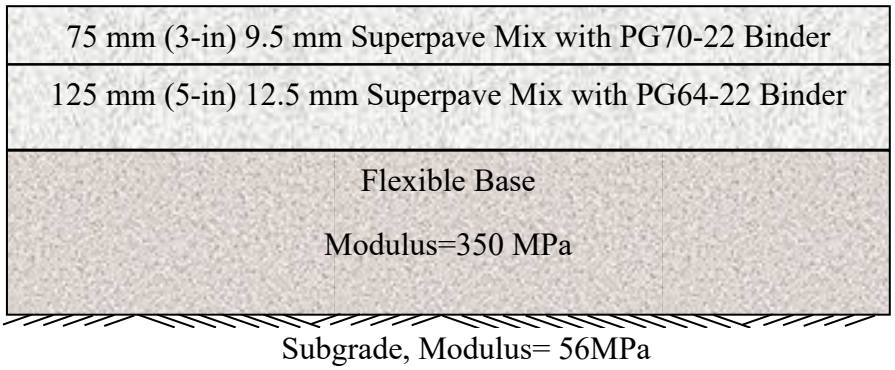

Figure 3. Illustration. Typical pavement structure used for this study.

These scenarios were simulated by the Texas Mechanistic-Empirical pavement design and analysis program (TxME) [10]. Figure 4 shows the corresponding TxME traffic input interface. In this program, the Wander Option inputs include the AV Percentage (0 means all AVs, 100 means all human-driven traffic ("regular"), a number between 0 and 100 means mixed traffic), AV Wander Standard Deviation, and AV Wander Distribution (Normal Distribution or Uniform Distribution). For human-driven traffic, the wander is always assumed to be normally distributed and the default standard deviation is 250 mm (10 in.).

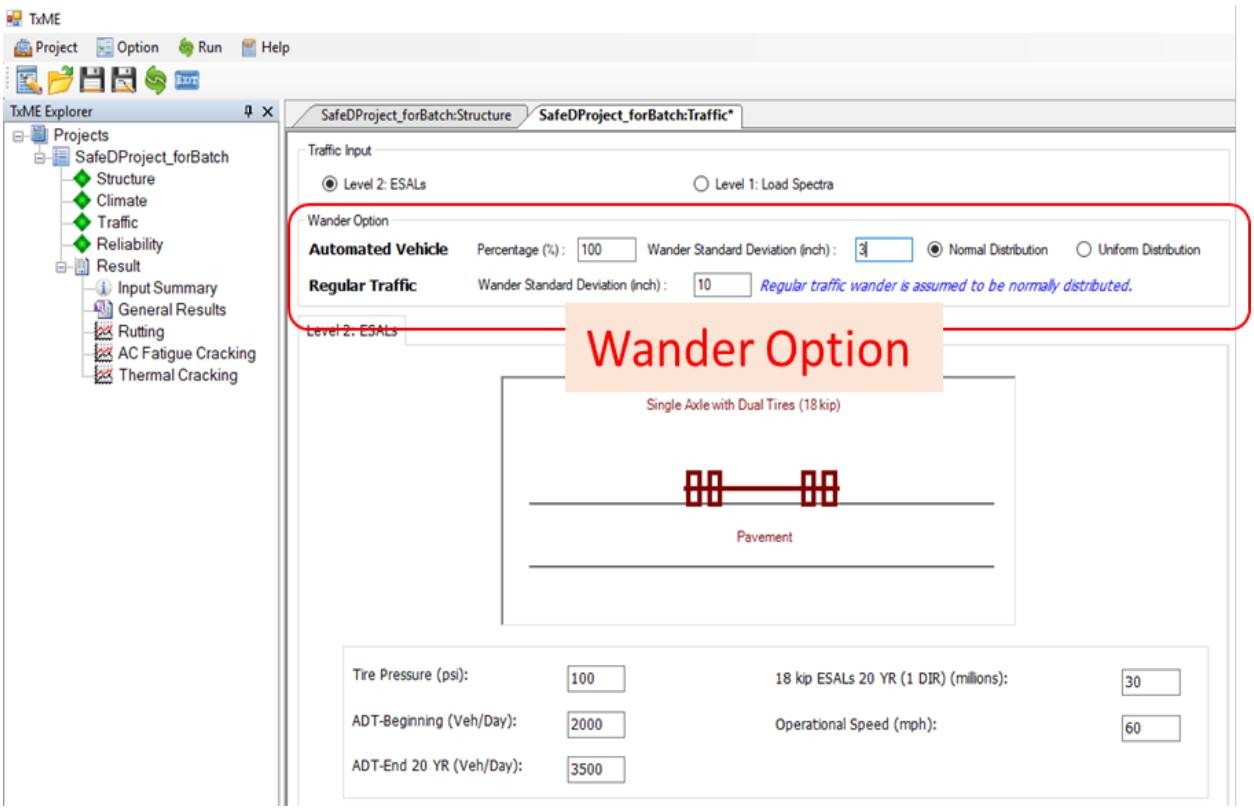

Figure 4. Screenshot. TxME traffic wander inputs.

Impact of AV on Hydroplaning-related Roadway Safety

Hydroplaning, especially dynamic hydroplaning, is a phenomenon in which a tire is completely separated from the pavement by a fluid layer, thus eliminating the friction between the tire and the pavement. As discussed previously, many accidents, deaths, and injures have been caused by hydroplaning [6]. Many factors influence hydroplaning potential, such as vehicle speed, tire pressure, tire tread depth, pavement texture, roadway geometry, and water film thickness (WFT). DOTs normally limit vehicle driving speed to prevent hydroplaning. Different models have been developed in the literature to predict hydroplaning speed (HPS). The widely accepted hydroplaning prediction model is the combined models (Equations 3 and 4) developed by Gallaway et al. [11] and Huebner et al. [12].

$$HPS = 26.04WFT^{-0.259} \text{ for } WFT < 2.4 \text{ mm (0.095 in.)} \quad (3)$$

$$HPS = 3.09A \text{ for } WFT \geq 2.4 \text{ mm (0.095 in.)} \quad (4)$$

where HPS is hydroplaning speed (mph), WFT is water film thickness (inches), and A is the greater of the values calculated using Equations 5 and 6.

$$A = \frac{10.409}{WFT^{0.06}} + 3.507 \quad (5)$$

$$A = \left(\frac{28.952}{WFT^{0.06}} - 7.817\right) MTD^{0.14} \quad (6)$$

where *MTD* is the mean texture depth measured with the silicon putty method (inches). For the most frequently used asphalt surface mix, the typical *MTD* value is around 0.91 mm (0.036 in.). Note that Equations 4, 5, and 6 are simplified forms of the original Gallaway equations with three assumptions: (1) tire tread depth is 2.38 mm (3/32 in.); (2) tire pressure is 167.5 kPa (24 psi); and, (3) ten percent spindown corresponds to full dynamic hydroplaning.

It is obvious that WFT is a crucial parameter to predict HPS. Many formulas [13] have been proposed to estimate WFT from different factors, such as plane length of flow path, rainfall intensity, MTD, and pavement cross slope (CS). Currently, pavement rut depth (RD) is not considered in all WFT formulas, although it affects the water flow path and accordingly WFT. Under this study, the authors employed a simple method to determine the maximum water depth (or WFT) within rutting zones. This method was originally recommended by Glennon [14]. Figure 5 illustrates the concept and the relationship among RD, pavement CS, and WFT. If the pavement CS is 0 percent, then the RD is equal to the WFT. On most roads, CS is larger than zero percent for drainage purposes in wet weather conditions. It often ranges from 0.5 percent to 2.5 percent (or more). For any roadway with a non-zero CS, the WFT can be estimated by the following equation:

$$WFT = RD - Half\ of\ rutting\ zone\ width \times CS \quad (7)$$

As long as CS is larger than 0 percent, only a portion of water that flows through a rutted zone will be retained due to pavement CS and gravity. The WFT is determined by the amount of retaining water in the rutted area, depending on RD, CS, and the width of the rutted area. The larger the RD, the larger the WFT, but WFT is always less than RD as long as CS is greater than 0 percent.

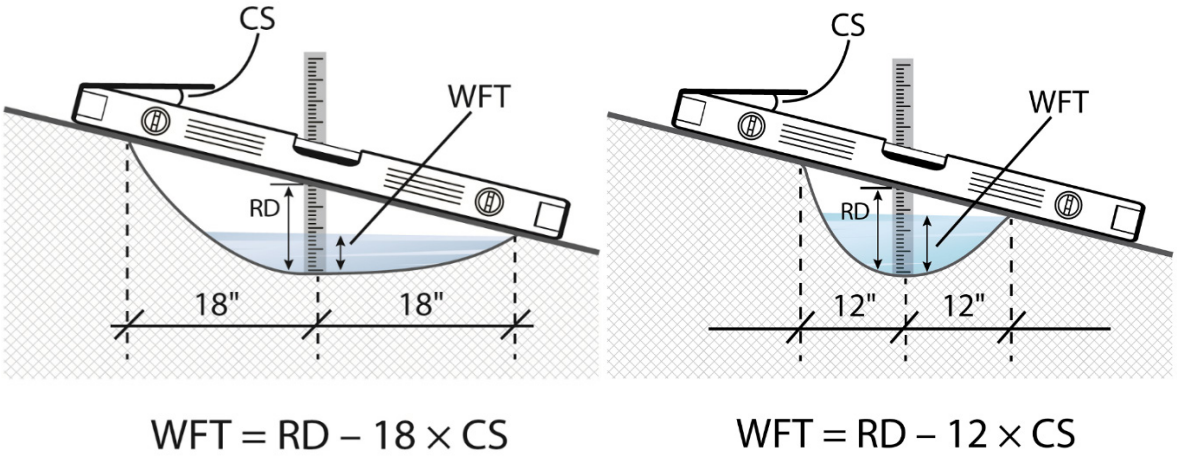

(a) human-driven truck traffic (b) AV traffic

Figure 5. Diagram. Pavement RD, CS, and maximum WFT.

As discussed previously, human-driven vehicles have greater lateral wandering, and a normal wheel path is around 0.9 m (3 ft) in either side of a travel lane [9]. In contrast, AVs wander much less, and the estimated wheel path is around 0.6 m (2 ft) in either side of a travel lane (see Figure 2). Thus, the width of an AV-rutted area is 0.3 m (1 ft) smaller than that of human-driven vehicles. Based on Equation 7, the WFT within an AV-rutted area is deeper than that of human-driven truck

traffic, as shown in Figure 5. The wider a rutted area is, the smaller the WFT is. Furthermore, the WFT is a function of CS as well: the larger the CS, the smaller the WFT. In the case of RD = 7.5 mm (0.3 in.) and CS = 1.5 percent, WFT is 0.75 mm (0.03 in.) for human-driven vehicles, but the corresponding WFT for the AVs is 3.00 mm (0.12 in.). From these WFT values, the HPSs estimated from Equations 3 through 6 for human-driven vehicles and AVs are 103 km/h (64 mph) and 77 km/h (48 mph), respectively. Therefore, the increased RD caused by a less-distributed wheel path results in a serious increase of hydroplaning risk. This is represented by a 26 km/h (16 mph) decrease in speed limit in order to avoid AV hydroplaning.

Optimization of AV Wandering to Improve Roadway Safety and Pavement Life

As noted previously, AVs are often equipped with very accurate lane keeping systems. Thus, it is possible to design lateral wandering patterns specifically for AVs that reduce the risk of hydroplaning and extend pavement life. It is envisioned that AV lateral wandering could be optimized through the lateral wandering width and associated distribution:

- Larger lateral wandering width: The use of a larger lateral wandering width has two benefits: (1) reducing the traffic load on a specific pavement location and accordingly increasing pavement cracking life and lessening RD, and (2) decreasing WFT (see Equation 7) by using the whole lane width (3.6 m/12 ft).

- Even distribution of traffic loading within the lateral wandering width: Both human-driven vehicles and AVs wander laterally following a normal distribution. For any normal distribution, regardless of standard deviation, the middle portion of wandering width always carries a higher number of loading passes than the other portions of the lane. This results in more cracking and deeper rutting in this portion of the lane. It is obvious that evenly distributing traffic load within the whole lane can lead to less damage to the pavement and little rutting.

With the consideration of these two aspects, a uniform distribution, as shown in Figure 6, is recommended as the optimal lateral wandering pattern for AVs. Note that the width of a regular 18-wheel truck is around 2.55 m (8.5 ft). For a 3.6-m (12 ft) traffic lane, the allowable, maximum lateral wandering width for AVs is 1.05 m (3.5 ft) from the left to right edge of the lane. With the optimal uniform distribution, the performance of the same pavement structure (Figure 3) under the same loading and environmental conditions was reanalyzed using TxME.

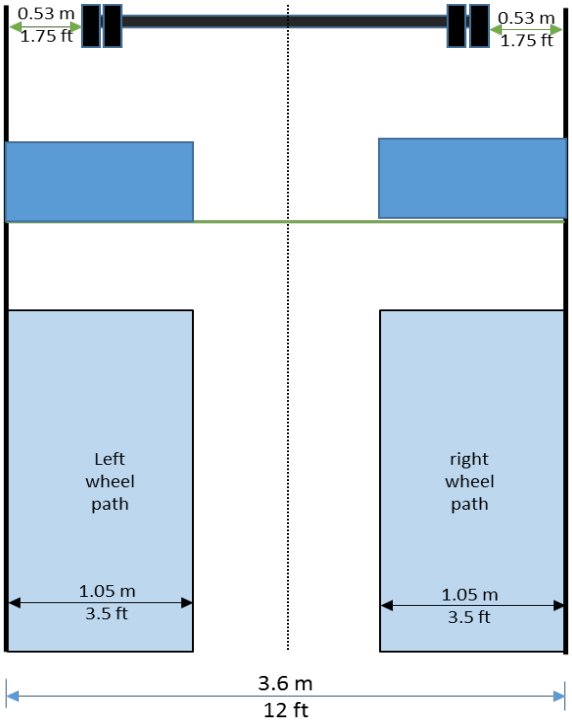

Figure 6. Illustration. Optimized AV lateral wandering pattern: uniform distribution.

Results

AV Lateral Wandering Pattern

Figure 7 shows an example of the measured AV lane following data. It is clear that the AV lateral wandering pattern can be described in a normal distribution with a standard deviation. Furthermore, the AV results, as expected, show little deviation from the center of the lane, with measured standard deviations ranging from 30 mm (1.2 in.) to 75 mm (3 in.). As reported in the literature [9], human-driven vehicles wander laterally with a standard deviation of 250 mm (10 in.). Comparing AVs with human drivers, the lateral wandering of AVs is at least 3 times narrower. As shown later, a smaller standard deviation in lateral wandering leads to more damage to the pavement and higher risk of hydroplaning.

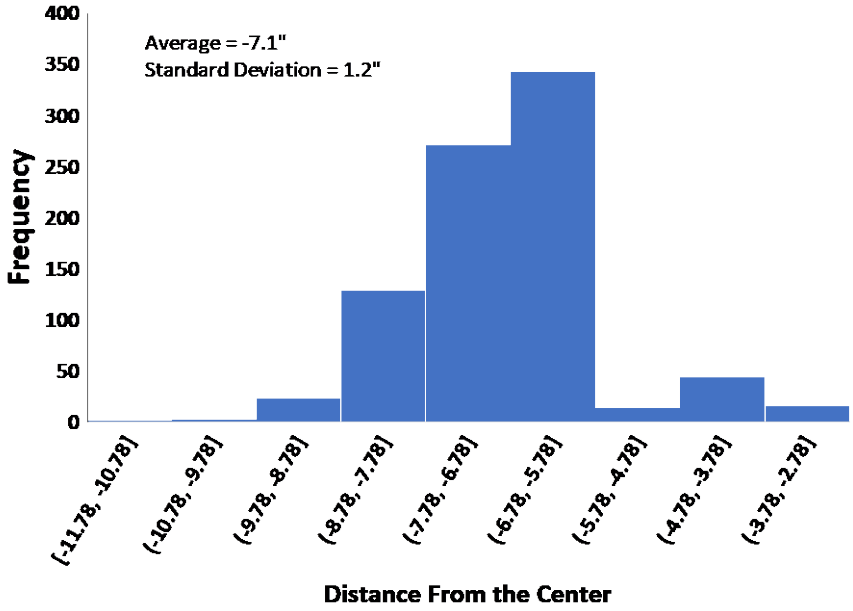

Figure 7. Chart. Example histogram of AV deviation from center of the lane in the test track.

Comparison of Pavement Life between Human-driven and AV Traffic

Figure 9 and Figure 9 show the development of pavement damage with time. Fatigue cracking is a type of structural damage to the pavement infrastructure. Generally, pavement failure (or pavement fatigue life) is defined as the time when the fatigue cracking area is 50 percent of the wheel path. Based on this definition, pavement fatigue lives for AVs and human-driven truck traffic (Figure 8) are 178 and 228 months, respectively. Apparently, AVs induce much more damage to the pavement and shorten its life by 22 percent. Furthermore, not only do AVs generate pavement rutting faster (see Figure 9), but the RD is also deeper than that of the human-driven truck traffic. If an RD of 7.5 mm (0.3 in.) is defined as a safety-related criterion [15], it takes AVs 96 months to generate a 7.5-mm RD, which is 39 percent sooner than the time for human-driven truck traffic of 157 months. These findings are consistent with the results reported by Rust et al. [3] and the accelerated pavement test (APT) results from the Virginia Tech Transportation Institute as described in Appendix A. Figure 10 shows a typical APT result. Note that if a smaller standard deviation were chosen, more pavement damage would be induced by AVs.

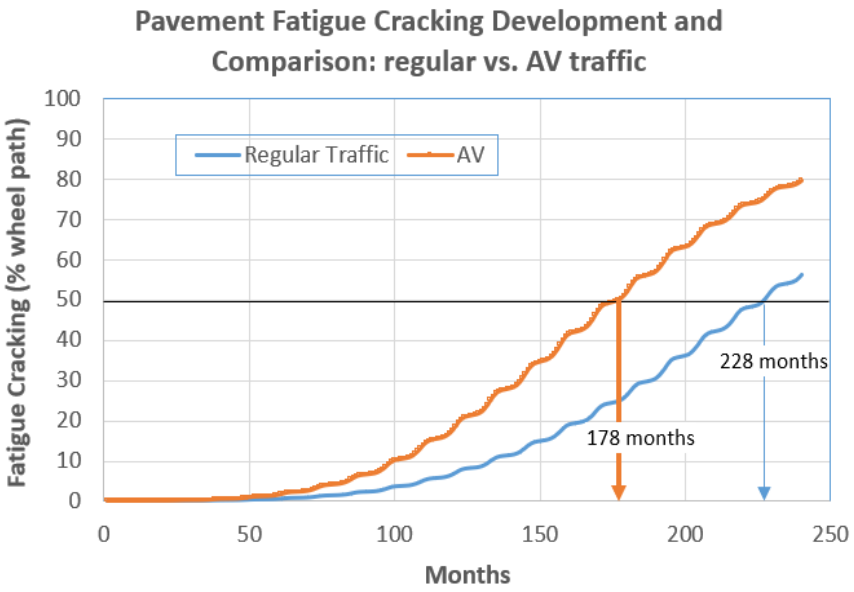

Figure 8. Graph. Fatigue cracking development for AV and human-driven traffic.

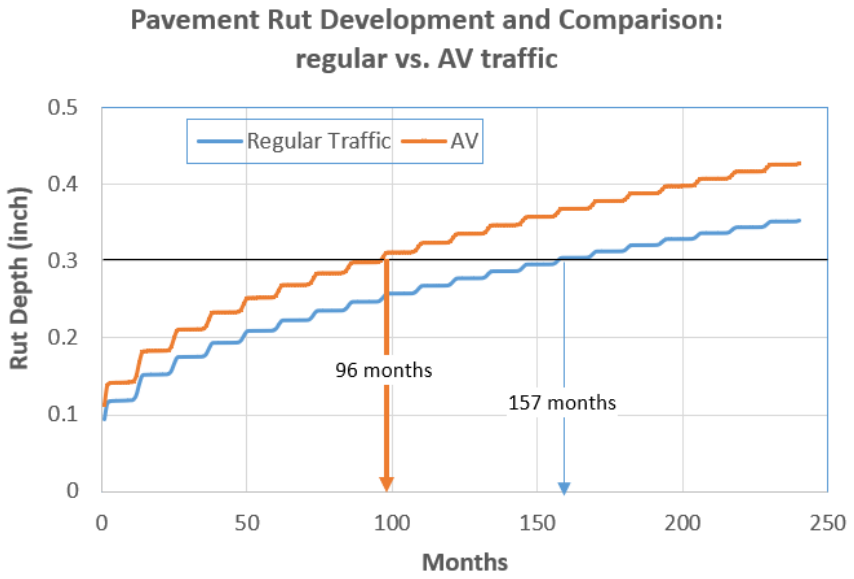

Figure 9. Graph. Rutting development for human-driven and AV truck traffic.

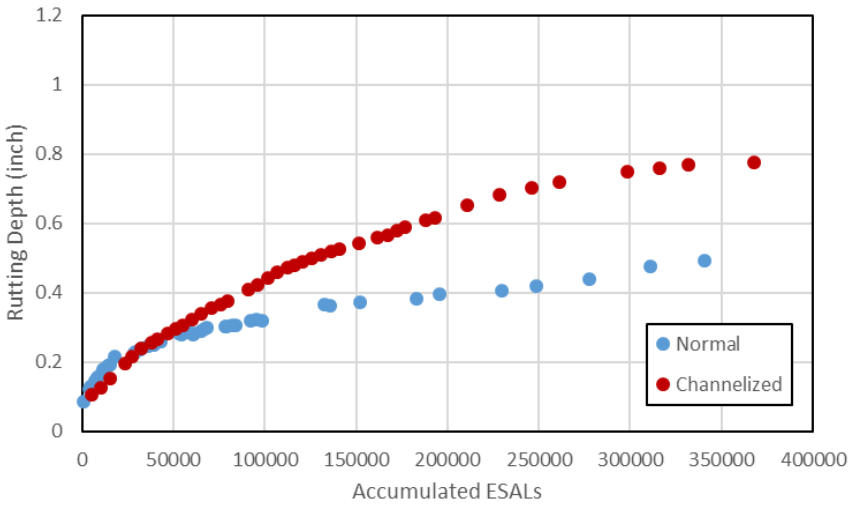

Figure 10. Graph. Rutting development under human-driven (or normal) and AV (channelized) wandering.

In the near future, both human-driven vehicles and AVs are anticipated to share pavement lanes. Thus, this study also investigated how mixed traffic will impact pavement lives. The fatigue cracking and rutting under different AV percentages were determined using TxME. Figure 11 and Figure 12 show the analysis results in terms of the fatigue life (defined as the number of months when the fatigue cracking area reaches 50 percent of the wheel path) and rutting life (defined as the number of months when the RD reaches 7.5 mm [0.3 in.]). Obviously, pavement performance in terms of both fatigue cracking and rutting grows worse as the percentage of AVs grows. Note that in this scenario, AV wandering is assumed to be normally distributed with a 75-mm (3-in.) standard deviation.

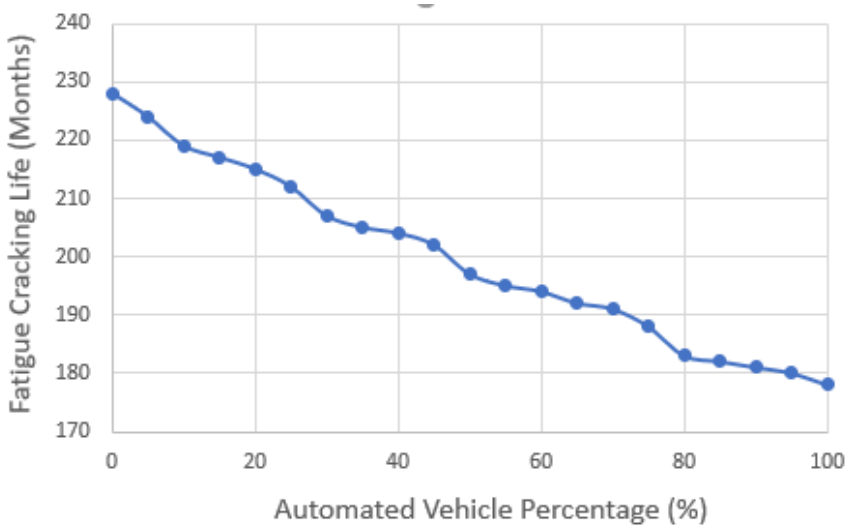

Figure 11. Graph. Fatigue cracking under mixed traffic.

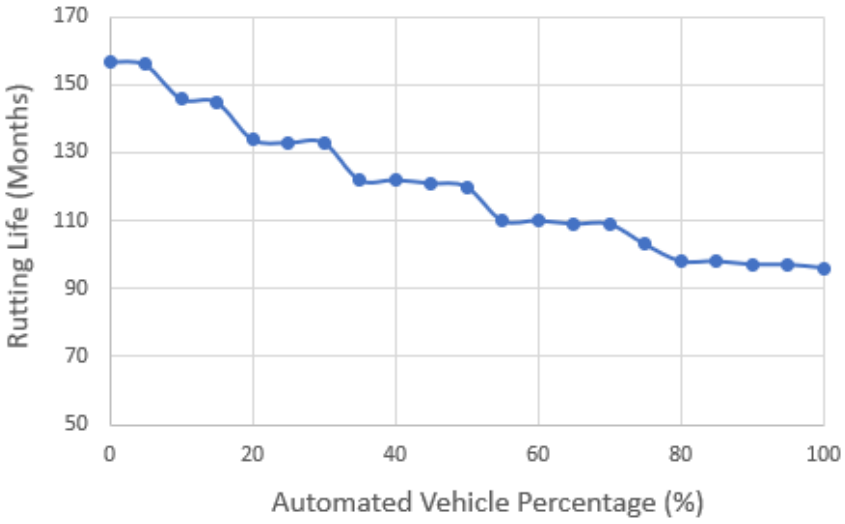

Figure 12. Graph. Rutting life under mixed traffic.

Comparison of Hydroplaning Potential between Human-driven and AV Traffic

Based on Equations 3 through 7, the authors further estimated the critical (or maximum tolerant) RDs for human-driven vehicles and AVs at different driving speeds and pavement CSs. Beyond the critical RD, there is a risk of hydroplaning for each specific driving speed. Table 1 details those critical RDs. Figure 13 and Figure 14 show the relationships between HPS and critical RDs. Again, in order to avoid potential hydroplaning, the speed limit for AVs must be reduced, which is contrary to the original purposes of deploying AVs. However, the impact of AVs on pavement life and hydroplaning safety could be altered from negative to positive with the changes recommended in the next section.

Table 1. Estimated Critical RDs for Human-driven Vehicles and AVs

Speed	Pavement CS (%)	Critical RD: Human-driven traffic with a standard deviation of 250 mm (10 in.) wandering	Critical RD: AVs with a standard deviation of 75 mm (3 in.) wandering
112 km/h (70 mph)	0.5	2.75 mm (0.11 in.)	1.25 mm (0.05 in.)
112 km/h (70 mph)	1.0	5.00 mm (0.20 in.)	2.00 mm (0.08 in.)
112 km/h (70 mph)	1.5	7.25 mm (0.29 in.)	2.75 mm (0.11 in.)
112 km/h (70 mph)	2.0	9.50 mm (0.38 in.)	3.50 mm (0.14 in.)
112 km/h (70 mph)	2.5	11.75 mm (0.47 in.)	4.25 mm (0.17 in.)
96 km/h (60 mph)	0.5	3.25 mm (0.13 in.)	1.75 mm (0.07 in.)
96 km/h (60 mph)	1.0	5.50 mm (0.22 in.)	2.50 mm (0.10 in.)
96 km/h (60 mph)	1.5	7.75 mm (0.31 in.)	3.25 mm (0.13 in.)
96 km/h (60 mph)	2.0	10.00 mm (0.40 in.)	4.00 mm (0.16 in.)
96 km/h (60 mph)	2.5	12.25 mm (0.49 in.)	4.75 mm (0.19 in.)
80 km/h (50 mph)	0.5	4.25 mm (0.17 in.)	2.75 mm (0.11 in.)
80 km/h (50 mph)	1.0	6.50 mm (0.26 in.)	3.50 mm (0.14 in.)

80 km/h (50 mph)	1.5	8.75 mm (0.35 in.)	4.25 mm (0.17 in.)
80 km/h (50 mph)	2.0	11.00 mm (0.44 in.)	5.00 mm (0.20 in.)
80 km/h (50 mph)	2.5	13.25 mm (0.53 in.)	5.75 mm (0.23 in.)

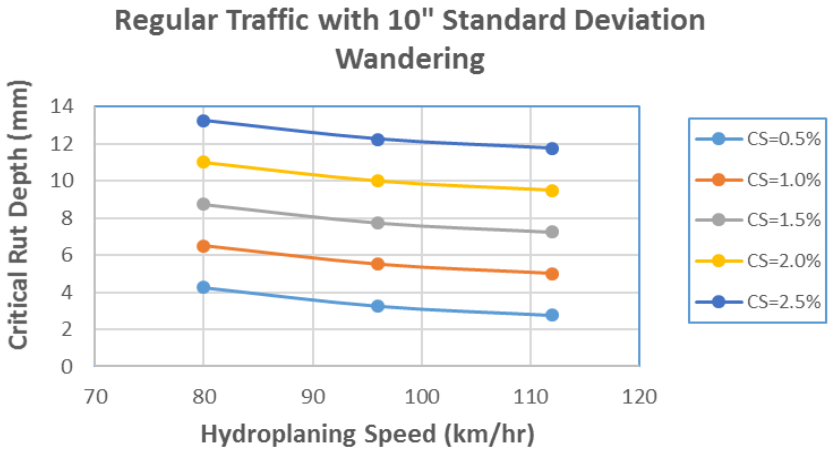

Figure 13. Graph. Critical RDs of human-driven traffic vs. HPS.

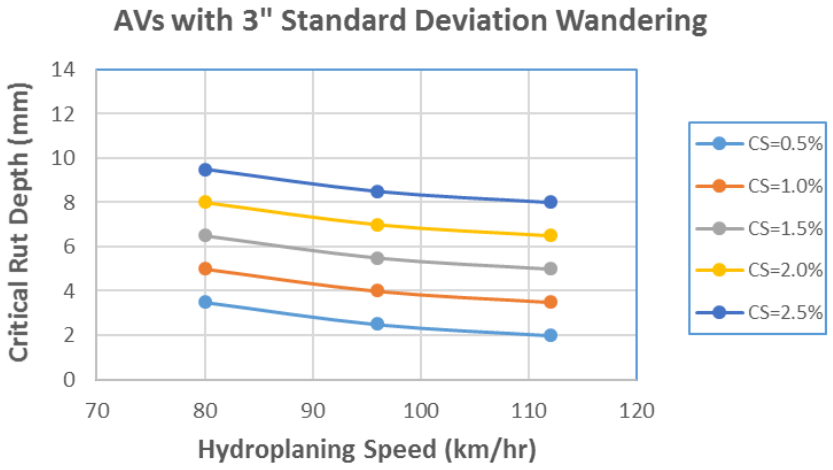

Figure 14. Graph. Critical RDs of AVs vs. HPS.

Pavement Life and Critical Rut Depths of Optimal Lateral Wandering Pattern

Figure 15 and Figure 16 show the predicted pavement fatigue cracking and rutting data when the AVs follow the optimal uniform distribution pattern. It can be seen that the optimal lateral wandering pattern of AVs (AV-Optimal) significantly delays pavement damage in terms of both rutting and fatigue cracking. The fatigue cracking life of AV-Optimal is 16 percent more than human-driven vehicles (265 months vs. 228 months), and 49 percent more than the AV with a narrow wandering pattern (265 months vs. 178 months). Comparing rutting life, AV-Optimal is 24 percent more than human-driven vehicles (194 months vs. 157 months) and 102 percent more than AVs with a narrow wandering pattern (194 months vs. 96 months).

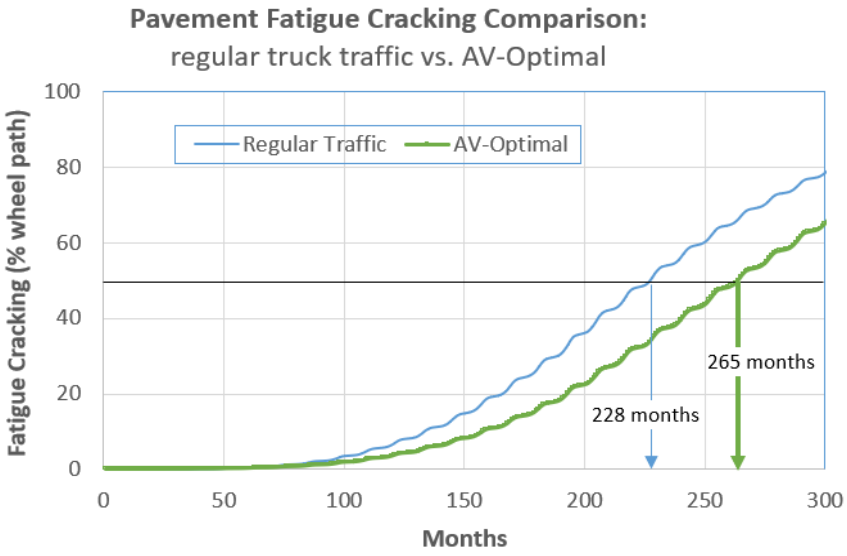

Figure 15. Graph. Fatigue cracking development for human-driven and AV-Optimal traffic.

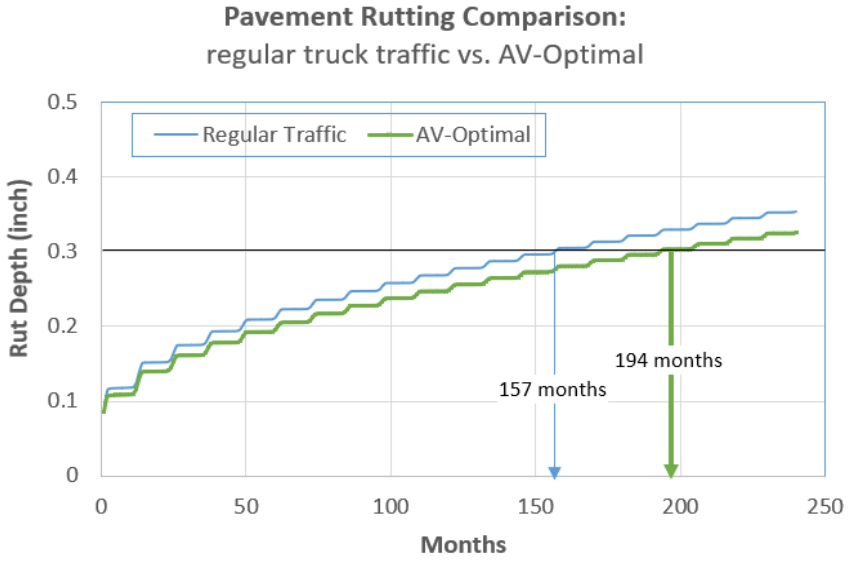

Figure 16. Graph. Rutting development for human-driven and AV-Optimal traffic.

Researchers also calculated the critical RDs based on the lateral wandering width of 1.05 m (3.5 ft) and Equations 3 through 7. The new critical RDs for AVs with optimal lateral wandering are tabulated in Table 2. For comparison purposes, Figure 17 plots the critical RDs for human-driven vehicles, AV narrow wandering (normally distributed, 7.5-mm [0.3-in.] standard deviation), and AV-Optimal (uniformly distributed) when the pavement CS equals 1.5%. It is clear that the optimal lateral wandering pattern can significantly reduce the risk of hydroplaning. Additionally, to maximize the positive benefit of AVs, current pavement lane width should be kept the same if not expanded so that AVs have enough space for lateral wandering.

Table 2. Estimated Critical RDs for AV-Optimal

Speed	Pavement CS (%)	Critical RD
112 km/h (70 mph)	0.5	3.13 mm (0.13 in.)
112 km/h (70 mph)	1.0	5.75 mm (0.23 in.)
112 km/h (70 mph)	1.5	8.38 mm (0.34 in.)
112 km/h (70 mph)	2.0	11.00 mm (0.44 in.)
112 km/h (70 mph)	2.5	13.63 mm (0.55 in.)
96 km/h (60 mph)	0.5	3.63 mm (0.15 in.)
96 km/h (60 mph)	1.0	6.25 mm (0.25 in.)
96 km/h (60 mph)	1.5	8.89 mm (0.36 in.)
96 km/h (60 mph)	2.0	11.50 mm (0.46 in.)
96 km/h (60 mph)	2.5	14.13 mm (0.57 in.)
80 km/h (50 mph)	0.5	4.63 mm (0.19 in.)
80 km/h (50 mph)	1.0	7.25 mm (0.29 in.)
80 km/h (50 mph)	1.5	9.89 mm (0.40 in.)
80 km/h (50 mph)	2.0	12.50 mm (0.50 in.)
80 km/h (50 mph)	2.5	15.13 mm (0.61 in.)

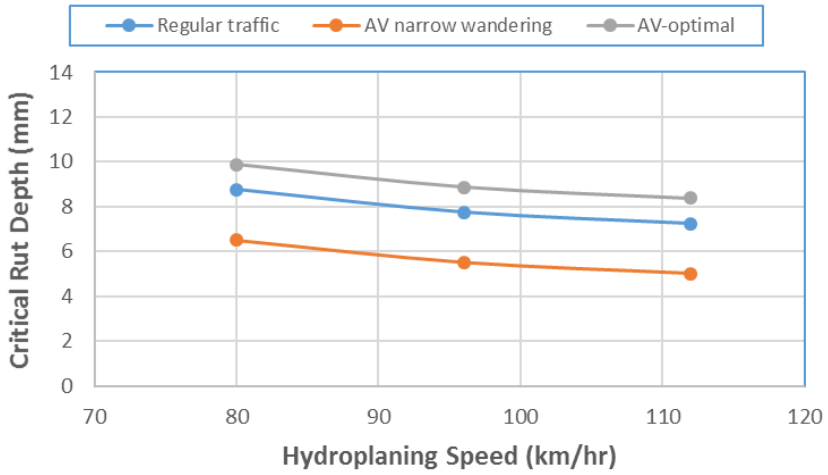

Figure 17. Graph. Comparison of critical RDs: regular traffic. vs. AVs with narrow wandering and AVs with optimal wandering (CS = 1.5%).

Figure 18 and Figure 19 show the mixed traffic analysis when the AVs follow the optimal wandering pattern. It is clear that pavement performance is better in terms of both fatigue and cracking as the percentage of AV-Optimal increases. Again, AV-Optimal wandering in this analysis is uniformly distributed within the 105-mm (42-in.) wheel path.

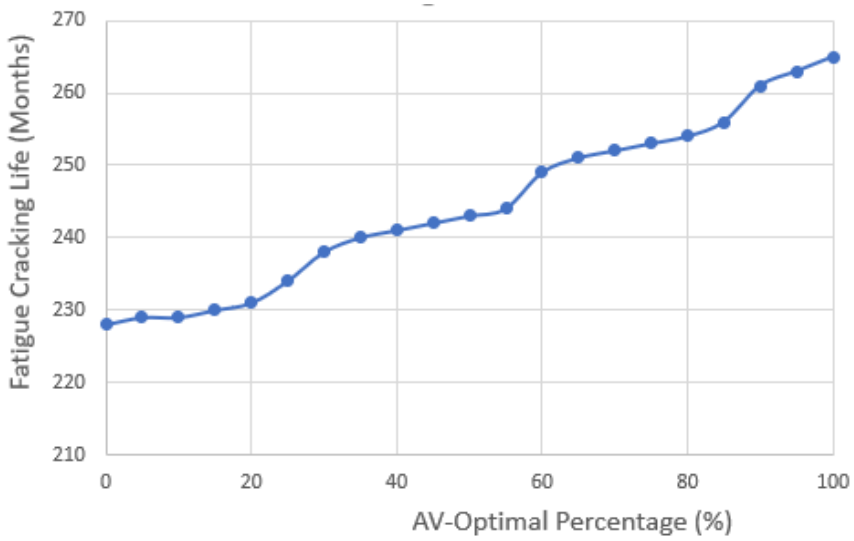

Figure 18. Graph. Fatigue cracking life for mixed traffic.

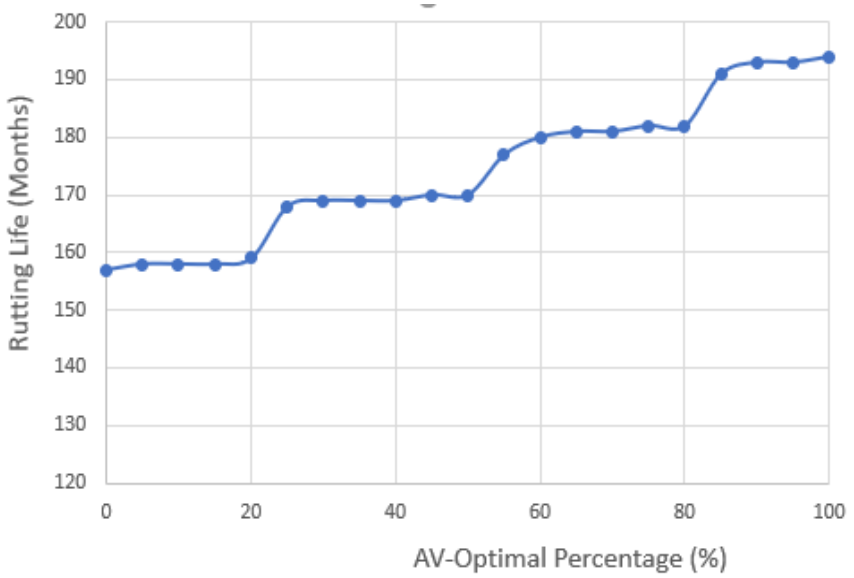

Figure 19. Graph. Rutting life for mixed traffic.

Discussion

This study evaluated the lateral wandering of AVs and associated negative impacts on pavement performance (fatigue cracking and rutting) and roadway safety (hydroplaning potential). The lateral wandering of AVs is much narrower than that of human-driven vehicles, which shortens pavement fatigue life and increases pavement RD. In addition, deeper RD increases the risk of hydroplaning for all vehicles. To address this issue, an optimal lateral wandering pattern, uniform lateral wandering, was recommended to eliminate the potential negative impacts of AVs on pavement life and roadway hydroplaning. The simulation results show that uniform lateral

wandering not only removes the negative effects but also prolongs pavement fatigue life, reduces rutting, and decreases hydroplaning potential.

This study employed a typical pavement structure located in Austin, Texas with 30-million ESAL traffic to demonstrate the comparison between human-driven and AV traffic. The predicted pavement lives and their relative differences may be different depending on pavement structure, weather, or traffic conditions, but the general trend is still valid.

Conclusions and Recommendations

Based on the results presented above, the following conclusions are offered:

- Although the wandering patterns of both AVs and human-driven vehicles can be described with a normal distribution, the lateral wandering of AVs is at least three times narrower than that of human-driven vehicles.

- The influences of the smaller lateral wandering of AVs on pavement rutting and fatigue life were analyzed with TxME. It was found that AVs shorten pavement fatigue life by 22 percent. Meanwhile, pavement RD increases 30 percent.

- Deeper RD obviously increases the risk of hydroplaning for all vehicles. In the case of RD = 7.5 mm (0.3 in.) and CS =1 .5%, the speed limit for avoiding hydroplaning for AVs has to be decreased by 26 km/h (16 mph) compared to human-driven vehicles. The critical RDs corresponding to different hydroplaning speeds and various pavement CSs were estimated in this study.

- The smaller lateral wandering of AVs compared to human-driven vehicles also leads to greater WFT within the rutted wheel path areas (Figure 8 and Equation 7), even if both types of vehicles induce the same RD. Thus, AVs have a higher risk of hydroplaning.

- An optimal lateral wandering pattern, uniform lateral wandering, is recommended to eliminate the potential negative impacts of AVs on pavement life and roadway hydroplaning. Not only does uniform lateral wandering remove the negative effects, but it also prolongs pavement fatigue life, reduces rutting, and decreases hydroplaning potential. The fatigue cracking life of the AV-Optimal pattern is 16 percent more than human-driven vehicles and 49 percent more than the AV-narrow wandering pattern. The rutting life of AV-Optimal is 24 percent more than human-driven vehicles and 102 percent more than the AV with narrow wandering pattern.

- Since both it is anticipated that human-driven vehicles and AVs will share pavement lanes together in the near future, this study also investigated how mixed traffic affects road safety and pavement life. The analysis showed that as the percentage of AVs without optimal wandering increases, pavement life shortens and the risk of hydroplaning increases. On the

contrary, if AVs are deployed with an optimal uniform distribution, pavement life increases and the risk of hydroplaning lessens as the percentage of AVs grows.

- To maximize the positive benefit of AVs, current pavement lane width, if not expanded, should be kept the same so that AVs have enough space for lateral wandering.

In order to further confirm and, more importantly, to implement the findings and conclusions of this study, the following research efforts are recommended:

- The measurement of lateral wandering in this study was based on multiple runs of one single AV in a straight tangent at a single driving speed of 20 mph. More measurements should be pursued with multiple AVs, specifically with heavy trucks at different driving speeds along roads with both tangent and curved sections.

- Collaboration with the AV industry is needed to practically implement the optimal uniform distribution lateral wandering pattern. The implementation could be for each AV alone or for AVs as a whole from a policy perspective.

- Another pavement-related safety issue is the influence of AVs on skid resistance. Significant efforts are necessary to evaluate how pavement skid resistance decreases with the applications of multiple AVs under different lateral wandering widths and various distribution patterns.

Additional Products

This section provides an overview of the products from this study related to education and workforce development, technology transfer, and data products. Interested readers may find Education and Workforce Development (EWD) and Technology Transfer (T2) products available for download as well as project updates on the project page on the Safe-D website. The final project dataset is located on the Safe-D Collection of the VTTI Dataverse.

Education and Workforce Development Products

Four Education and Workforce Development Products were developed for this project each of which is described below. At the time this report was submitted, all items had been completed.

1. Mr. Aman Sharma, a graduate student at Texas A&M University, participated in the early stage of this project. The project helped Mr. Sharma understand the factors behind rut-hydroplaning and the contribution of each factor to road accidents.

2. Findings from this study were presented to an international audience at the Transportation Research Board Annual Meeting held on January 13–17, 2019. Project principal investigator Fujie Zhou presented a paper under the title, “Optimization of Lateral

Wandering of Automated Vehicles to Reduce Hydroplaning Potential and to Improve Pavement Life."

3. Two animations and corresponding descriptions explain the differences in RD caused by different vehicle lateral wandering patterns and how hydroplaning occurs.
4. A PowerPoint presentation, entitled "Optimization of Lateral Wandering Pattern of Automated Vehicles to Reduce Hydroplaning Potential and to Improve Pavement Life," was developed that can be used as part of college classes such as "Introduction of Transportation Engineering." The presentation describes characteristics of AVs and the impact of AVs on pavement life and hydroplaning potential. It also presents the optimized lateral wandering pattern for automated vehicles, which improves both pavement life and safety by reducing hydroplaning potential.

Technology Transfer Products

The project report will be the primary product of this study. It will be posted on at least three platforms: the Safe-D website, the TTI publications catalog, and the TRID database.

A white paper was published on the TTI website.

A summary research paper of these findings was submitted and accepted for publication in the journal *Transportation Research Record*.

Data Products

Two data files are available on the Safe-D Collection of the VTTI Dataverse at https://doi.org/10.15787/VTT1/1QXWSN in Excel format. The data files show the pavement life prediction results for different scenarios such as AV traffic, human-driven traffic, AV-optimal traffic, and mixed traffic.

References

1. Fagnat, D. J., and K. M. Kockelman. Preparing a Nation for Autonomous Vehicle: Opportunities, Barriers and Policy Recommendations. *Transportation Research Part A: Policy and Practice*, Vol. 77, 2015, pp. 167-181.

2. Monismith, C. L. *On the Road Again*, https://www.ce.berkeley.edu/sites/default/files/news/93/Monismith_California%202%204.pdf, accessed on July 20, 2018.

3. Rust, F. C., J. T. Harvey, B. J. Verhaeghe, W. Nokes, and J. Van Kirk. Fatigue and Rutting Performance of Conventional Asphalt Bitumen-Rubber Asphalt Under Accelerated Trafficking, *Proceedings of the 6th Conference on Asphalt Pavements for Southern Africa*, South Africa, October 1994, pp.199-215.

4. Noorvand, H., G. Karnati, and B. S. Underwood. Autonomous Vehicles: Assessment of the Implications of Truck Positioning on Flexible Pavement Performance and design, *Transportation Research Record: Journal of the Transportation Research Record*, 2017. 2640: 21-28.

5. Wu, R., and J. Harvey. Evaluation of the Effect of Wander on Rutting Performance in HVS Tests, *Proceedings of the 3rd International Conference on Accelerated Pavement Testing*, Spain, 2008.

6. Herrman & Herrman, P.L.L.C. Safe Driving on Wet Roads: Dangers of Hydroplaning, https://www.herrmanandherrman.com/blog/safe-driving-wet-roads-dangers-hydroplaning/, accessed on July 29, 2018.

7. Girshick, R., J. Donahue, T. Darrell, and J. Malik. Rich Feature Hierarchies for Accurate Object Detection and Semantic Segmentation. *Proceedings of the IEEE Conference on Computer Vision and Pattern Recognition,* 2014, pp. 580-587.

8. Bojarski, M., D. Del Testa, D. Dworakowski, B. Firner, B. Flepp, P. Goyal, and X. Zhang. *End to End Learning for Self-driving Cars*, 2016, *arXiv preprint arXiv:1604.07316*.

9. AASHTO. *Mechanistic-Empirical Pavement Design Guide – A Manual of Practice*, American Association of State Highway and Transportation Officials (AASHTO), Washington, D.C., 2008.

10. Hu, S., F. Zhou, and T. Scullion. *Development of Texas Mechanistic-Empirical Flexible Pavement Design System (TxME)*, FHWA/TX-0-6622-2, Texas A&M Transportation Institute, College Station, Tx, 2014.

11. Gallaway, B. M., D. L. Ivey, G. Hayes, W. Ledbetter, R. Olson, D. Woods, and R. Schiller. *Pavement and Geometric Design for Minimizing Hydroplaning Potential*, FHWA-*RD-79-31*, Texas Transportation Institute, College Station, Tx, 1979.

12. Huebner, R., J. Reed, and J. Henry. Criteria for Predicting Hydroplaning Potential, ASCE *Journal of Transportation Engineering*, Vol. 112, 1986, pp. 549-553.

13. Jayasooriya, W., and M. Gunaratne. Evaluation of Widely Used Hydroplaning Risk Prediction Methods Using Florida's Past Crash Data, *Transportation Research Record: Journal of the Transportation Research Board,* 2014. *2457*: 140-150.

14. Glennon, J. C. Roadway Hydroplaning - Measuring Pavement Wheel Rut Depths to Determine Maximum Water Depths, http://www.crashforensics.com/papers.cfm?PaperID=55, accessed on March 29, 2018.

15. Fwa, T. F., H. R. Pasindu, and G. P. Ong. Critical Rut Depth for Pavement Maintenance Based on Vehicle Skidding and Hydroplaning Consideration, *Journal of Transportation Engineering*, Vol. 128, No. 4, 2012.

Appendix A – The Impact of Lateral Positioning Pattern on Pavement Rutting Under Accelerated Pavement Testing

Abstract

An Accelerated Pavement Testing (APT) experiment was conducted on to assess the impact of lateral positioning pattern of traffic load on HMA pavement. The experiment measured and compared the rutting development at the pavement surface under two loading patterns: one is normal and the other is a channelized pattern within only 4-inch wandering.

Pavement surface deformation was scanned using laser profiler. Rutting depth was calculated for each transverse plane and averaged within the middle area with constant speed. The result shows that channelized lateral positioning pattern with 4-inch wandering will bring in 57% more rutting compared to the normal distribution.

Introduction

Automated vehicles (AV) and connected vehicles (CV) are the research and application focus in transportation, and may be put into practice in near future. If so, the traffic flow will be quite different from the traditional one, and the design of traffic infrastructure should be adjusted accordingly. One significant difference between the AV/CV traffic and traditional traffic flow is the lateral positioning pattern. The lateral position of manually driven vehicles are influence by numerous factors (Luo and Wang 2013), including weather, visibility, horizontal curve, and traffic condition and so on, and follows normal distribution generally. In contrast, AV positions itself within a lane by keeping a fixed distance from the lane marker or some other reference, which will form a channelized traffic flow with very small wandering. Theoretically such concentrated traffic loading will induce a lot of deterioration to pavement structures. However, few previous studies can be found to address this issue.

In 2015, VDOT initiated an Accelerated Pavement Testing (APT) program at Virginia Tech Transportation Institute (VTTI), employing a Heavy Vehicle Simulator (HVS) as its technological centerpiece. In 2017, the SAFE-D National University Transportation Center (UTC) initiated a study to explore the impact of AV/CV lateral positioning pattern on pavement rutting performance. A test lane (lane 4) in VDOT's APT facility was used to conduct experiments. The main objective of the report is to summarize the research, compare the pavement rutting status under two different lateral positioning patterns of wheel load, and explore the impact of channelized traffic on pavement rutting performance.

Method

Test Sections

Six test lanes were built in 2015 with specific research purposes as the first stage of the APT program. The lane 4 with dense-graded surface mixtures is chosen to conduct APT experiment in this study. Lane 4 is divided into two test sections (4A and 4B) as replicates. The structure was built over a 27-inch subgrade layer placed over a rigid foundation. It features a 7-inch 21-B aggregate subbase, a 4-inch IM-19.0 mm (normal maximum aggregate size, NMAS) intermediate mixture base layer, and a 3-inch thick 9.5-mm (NMAS) dense-graded surface layer. The structure of pavement sections is shown in Figure A-1.

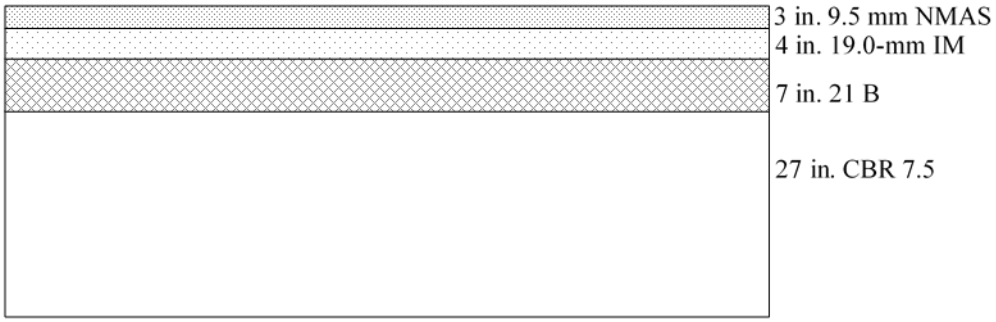

Figure A-1. Pavement structure in Lane 4.

Equipment

The HVS used at the Virginia APT facility is a model Dynatest Mark VI (shown in Figure A-2), which is the newest model among the Dynatest HVS systems. This model allows testing longer pavement sections at higher speeds than previous versions. It has an available test wheel speed of up to 12.4 mph (± 2 mph) for loads that range from 6,750 lbf to 22,500 lbf and can achieve 24,000 bi-directional passes or 12,000 uni-directional passes in 24 hours (Cooke 2015). The unit also contains an environmental chamber that maintains a relatively constant temperature at the loaded area. The pavement surface is heated with infrared heaters located along the edge of the test lane within the environmental chamber.

Figure A-2. Dynatest Mark VI Heavy Vehicle Simulator.

A laser profiler mounted on the HVS carriage (shown in Figure A-3) was used to scan the pavement surface and measure the vertical permanent deformation at the pavement surface. The rut depth measurements can be collected across the full width of the wheel path for a distance of 80 inches (40 inches on either side of the center of the wheel path) and for a distance of 17 feet and 8 inches. The spacing of the measurements is 4 inches in the longitudinal direction, and 1 inch in the transverse direction.

Figure A-3. Laser profiler mounted on HVS carriage.

Experiment

Accelerated pavement testing was conducted to evaluate pavement rutting performance under different lateral positioning patterns. Two patterns are used in this study as shown in Figure A-4: one is channelized with only 4-inch wandering, and one is the normal distribution specified by the Mechanistic-Empirical Pavement Design Guide (MEPDG).

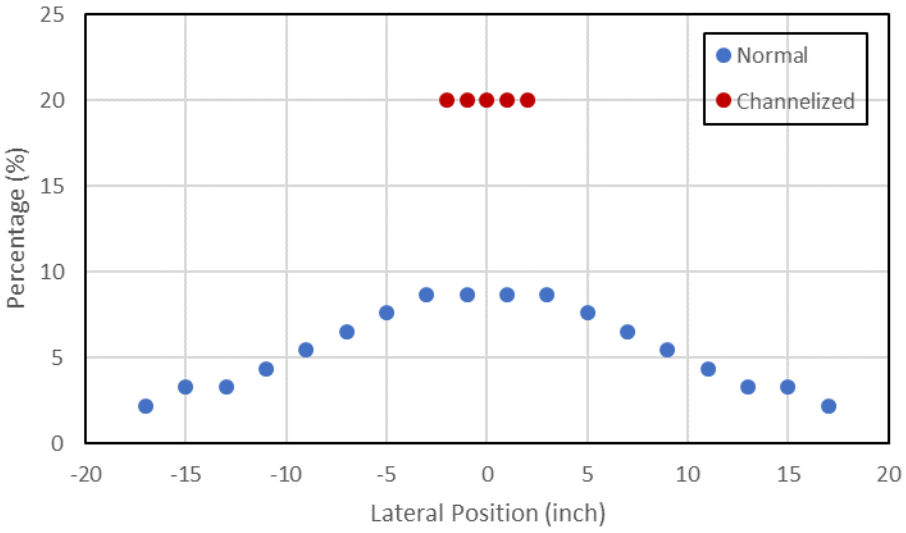

Figure A-4. Lateral positioning patterns

During each test, the HVS operated continuously with the exception of regular daily maintenance and occasional repairs. The temperature of the surface layer was held at 104°F as monitored by a thermocouple embedded at a depth of 2 inches from the surface. The loading sequence consisted of applying a number of passes at progressively higher load levels of 9,000 lbf, 12,000 lbf, and 15,000 lbf. The loading was applied through a dual tire assembly, with 11.00R22.5 tires inflated at 110 psi. The assembly was running uni-directionally at a constant speed of 4 mph.

The 9,000 lbf load level was intended to simulate half of an 18,000 lb standard axle load. The loading and repetitions were transformed into ESALs using the conversion shown in Equation 1:

$$ESALs = \left(\frac{wheel\ load}{9{,}000}\right)^{4.2} \quad \text{(A-1)}$$

Using Equation A-1, one pass of the 9,000, 12,000, and 15,000 lb load level was equivalent to 1.00, 3.35, and 8.55 ESALs, respectively. The ESAL progressions for the four test cells are summarized in Figure A-5.

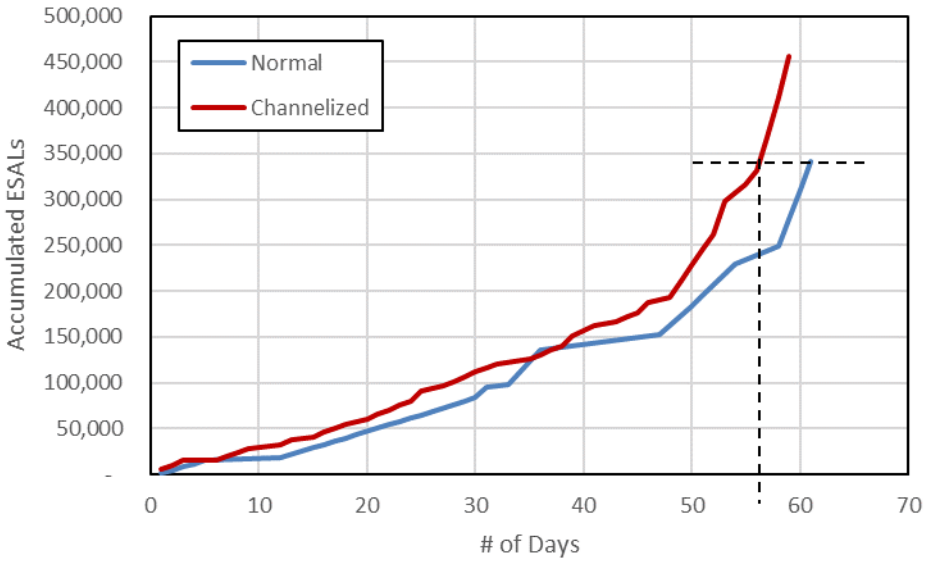

Figure A-5. Loading charts in the experiments.

As shown in Figure A-5, the experiment under channelized loading pattern reached the same ESALs as in the end of the experiment under normal pattern on the 56th day. So the following analysis represents the rutting development from the first day to the 56th day when referred to the experiment under channelized loading pattern.

The laser profiler was mounted on the carriage of HVS, and scanning the surface of test bed every day after regular maintenance of HVS. One scanned surface is shown in Figure A-6 for demonstration purposes. The daily rutting profile shows the deformation of the pavement surface and is used to calculate the rutting depth.

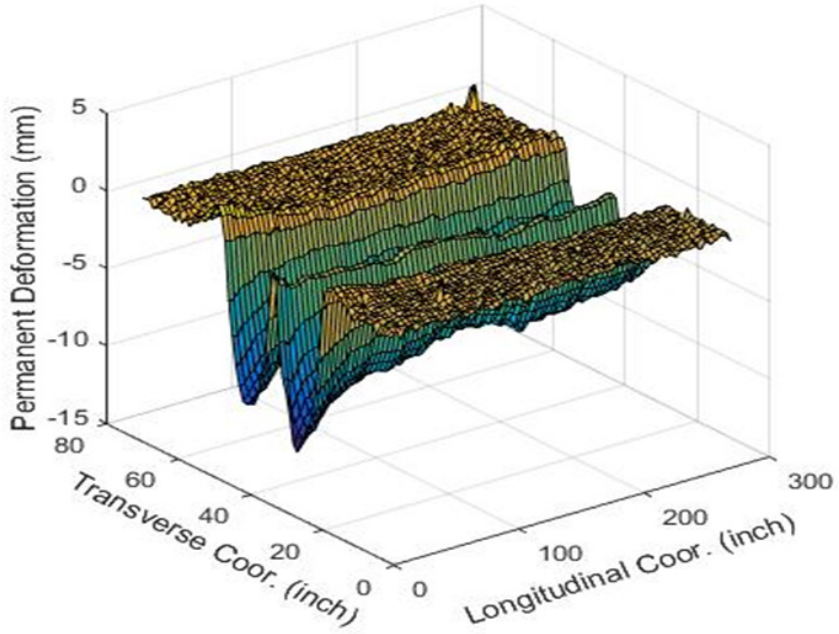

Figure A-6. Example of the measurements from laser profiler.

Results

The permanent deformation at pavement surface unbalance vehicles and lead to water accumulation, and affect driving comfort and safety as a result. The laser profiler mounted on HVS carriage were used in this study to measure the permanent deformation at the surfaces of testbed.

The laser profiler can scan the whole surface as shown in previous section (Figure A-6). Figure A-7 describes the calculation of rutting depth so that scholars can quantify pavement permanent deformation for each transverse plane. Each point in the scanned surface represent the surface vertical permanent deformation at the location from the original level. Rutting depth incorporates the lifts and the shape of deformation in the transverse plane into the calculation.

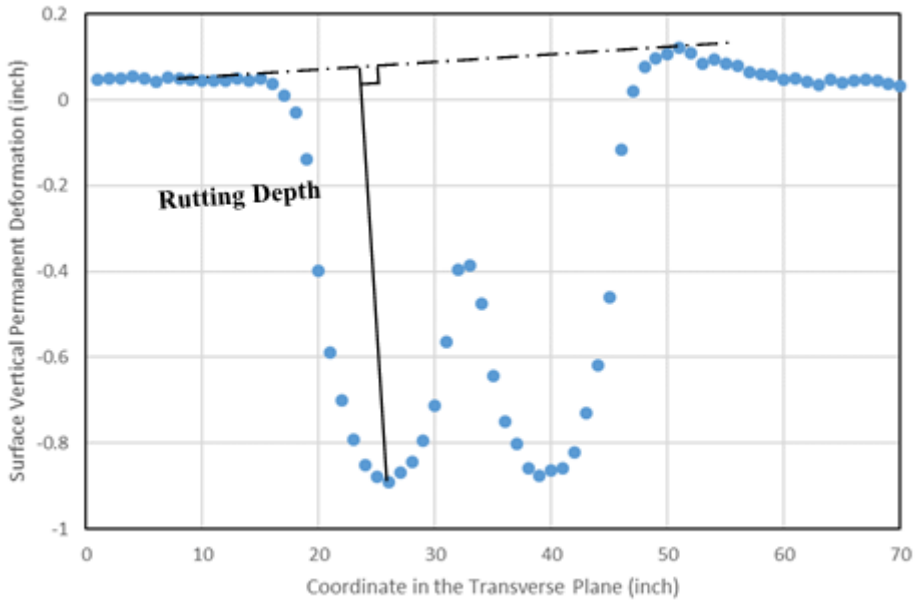

Figure A-7. Calculation of rutting depth based on the scanned surface deformation.

As indicated in Figure A-7, each transverse plane has a rutting depth. The distribution of rutting depth along the longitudinal direction is shown in Figure A-8. Due to the time limit, the experiment under channelized lateral pattern was conducted using the short beam of HVS, and then the last one third of pavement surface in longitudinal direction can't be scanned due to the direction and location of the profiler. So the number of transverse planes under channelized pattern is much smaller than those under normal pattern as shown in Figure A-8. During each pass, the wheel on HVS accelerates first, then runs with a constant speed (4 mph), and then decelerates until stop at the end of the track. To obtain the rutting performance of test cells under constant speed, the rutting depths were averaged in the middle part for every day throughout the experiments. The averaged rutting depth is plotted for everyday in Figure A-9 to compare the rutting performance of pavement under the two loading patterns.

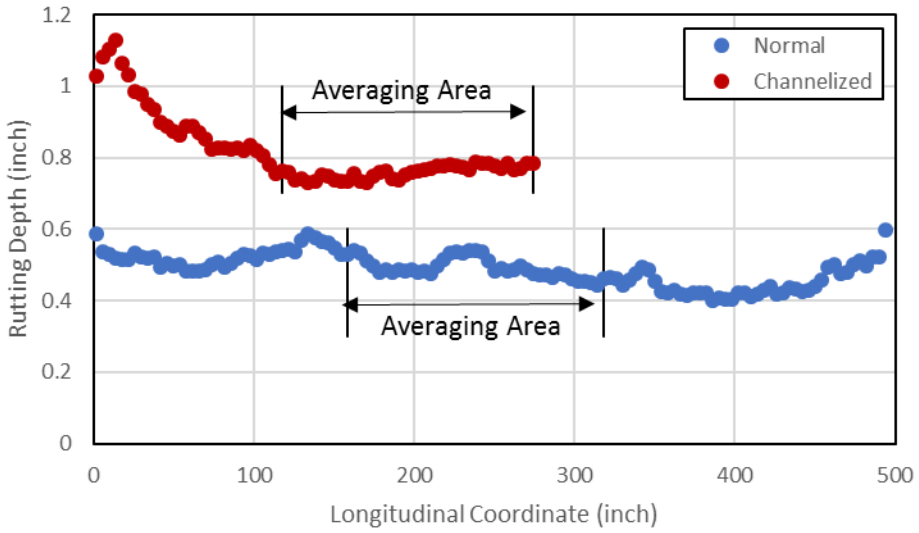

Figure A-8. Distribution of rut depth along the longitudinal direction.

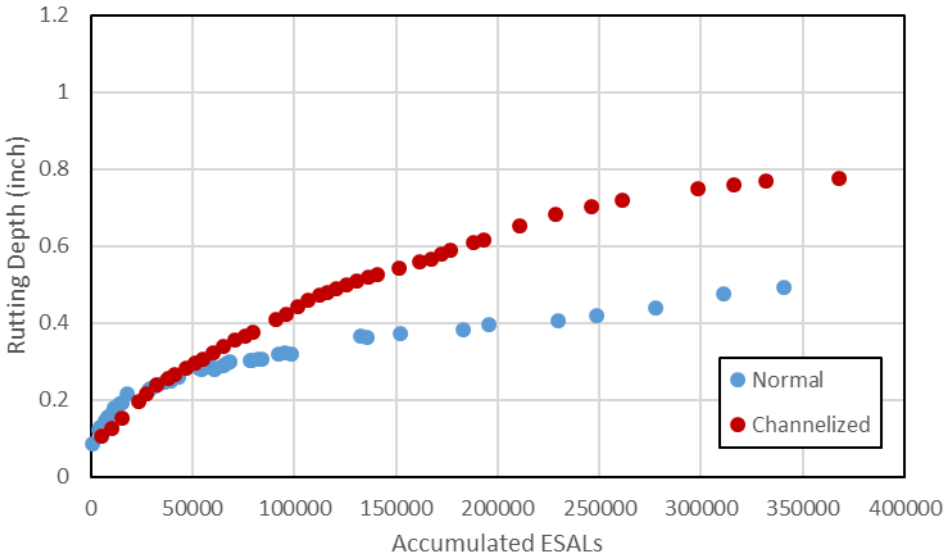

Figure A-9. Development of Rutting Depth under the two loading patterns.

Figure A-9 shows that the rutting depths under the two loading positioning patterns were quite different. The channelized pattern with a four-inch wandering will produce 57.1% more rutting compared to the normal pattern. If the traffic load is further channelized with even smaller wandering, such as one-inch or zero wandering, then the rutting will be much bigger and would totally break the functionality of pavement structure.

Conclusions

This report documents the results of an APT experiment to assess the impact of lateral positioning pattern of traffic load on HMA pavement. The experiment measured and compared the rutting development at the pavement surface under two loading patterns: one is the normal

distribution suggested by MEPDG, and the other is a channelized pattern within only 4-inch wandering.

Pavement surface deformation was scanned using laser profiler. Rutting depth was calculated for each transverse plane and averaged within the middle area with constant speed. The result shows that channelized lateral positioning pattern with 4-inch wandering will bring in 57% more rutting compared to the normal distribution.

Considering the potential widely use of automatic vehicles, public traffic can be further channelized and the general wandering could be smaller than 4 inches. If so, the rutting depth in pavement will be much higher, and the functionality of transportation infrastructure could be seriously affected in a short time. Based on the result of this study, it is recommended that future studies be conducted to explore the performance of various pavement structures under channelized lateral positioning pattern.

References

Cooke, B. HVS MK VI I VDOT User Manual. Dynatest Consulting, DH6G820000100, 2015.

Luo, W. and K. C. P. Wang (2013). Wheel Path Wandering Based on Field Data. Airfield and Highway Pavement 2013: 506-515.